

AAPM/RSNA Physics Tutorial for Residents: Topics in CT

Radiation Dose in CT¹

Michael F. McNitt-Gray, PhD

This article describes basic radiation dose concepts as well as those specifically developed to describe the radiation dose from computed tomography (CT). Basic concepts of radiation dose are reviewed, including exposure, absorbed dose, and effective dose. Radiation dose from CT demonstrates variations within the scan plane and along the z axis because of its unique geometry and usage. Several CT-specific dose descriptors have been developed: the Multiple Scan Average Dose descriptor, the Computed Tomography Dose Index (CTDI) and its variations (CTDI₁₀₀, CTDI_w, CTDI_{vol}), and the dose-length product. Factors that affect radiation dose from CT include the beam energy, tube current–time product, pitch, collimation, patient size, and dose reduction options. Methods of reducing the radiation dose to a patient from CT include reducing the milliamperere-seconds value, increasing the pitch, varying the milliamperere-seconds value according to patient size, and reducing the beam energy. The effective dose from CT can be estimated by using Monte Carlo methods to simulate CT of a mathematical patient model, by estimating the energy imparted to the body region being scanned, or by using conversion factors for general anatomic regions. Issues related to radiation dose from CT are being addressed by the Society for Pediatric Radiology, the American Association of Physicists in Medicine, the American College of Radiology, and the Center for Devices and Radiological Health of the Food and Drug Administration.

©RSNA, 2002

Abbreviations: CTDI = Computed Tomography Dose Index, DLP = dose-length product, ICRP = International Commission on Radiological Protection

Index terms: Computed tomography (CT), radiation exposure • Dosimetry • Radiations, exposure to patients and personnel • Radiations, measurement

RadioGraphics 2002; 22:1541–1553 • Published online 10.1148/rg.226025128

¹From the Department of Radiology, David Geffen School of Medicine, University of California, Los Angeles, Box 951721, Los Angeles, CA 90095-1721. From the AAPM/RSNA Physics Tutorial at the 2001 RSNA scientific assembly. Received July 18, 2002; revision requested August 13 and received August 29; accepted August 30. **Address correspondence to** the author (e-mail: mmcnittgray@mednet.ucla.edu).

©RSNA, 2002

Introduction

Although computed tomography (CT) represents only a small percentage of radiologic examinations, it results in a significant portion of the effective radiation dose from medical procedures (1). With the increasing use of CT for screening procedures (2) and advances in scanner technology, the trend for increased numbers of procedures performed with this imaging modality may increase. Although CT is clearly providing many clinical benefits, the motivation to understand radiation dose in general as well as the specific concepts related to CT grows with the prevalence of this modality.

The purpose of this article is to review basic radiation dose concepts as well as those specifically developed to describe the radiation dose from CT. This involves describing the basic concepts of exposure, dose, and effective dose and showing how these are defined or estimated for CT. After the definitions are given, the effects of various technical CT factors on radiation dose are described. Next, some typical values for each dose parameter are given for a few select imaging protocols. Finally, some relevant resources and current activities are discussed.

Radiation Dose

Measures: General Definitions

Exposure

The term *exposure* (3) describes the ability of x rays to ionize air. It is measured in roentgens (R); this unit is defined as the quantity of x rays that produces 2.580×10^{-4} C of charge collected per unit mass (kilograms) of air at standard temperature and pressure (STP): $1 \text{ R} = 0.000258 \text{ C/kg}$ air. This term refers to the concentration, in air, of radiation at a specific point and is the ionization produced in a specific volume of air. It is typically measured with an ionization chamber and an electrometer. It essentially describes how much ionization is present in the volume, but it does not tell how much energy is absorbed by the tissues being irradiated.

Absorbed Radiation Dose

Absorbed radiation dose (3), often referred to as *radiation dose*, describes the amount of energy absorbed per unit mass at a specific point. It is measured in grays ($1 \text{ Gy} = 1 \text{ J/kg}$) or rads ($1 \text{ rad} = 100 \text{ erg/g}$). The conversion between rads and grays is $100 \text{ rad} = 1 \text{ Gy}$. Absorbed dose essentially describes how much energy from ionizing

radiation has been absorbed in a small volume centered at a point; it does not describe where that radiation dose is absorbed or reflect the relative radiosensitivity or risk of detriment to those tissues being irradiated.

Effective Dose

Effective dose (3–5) (formerly referred to as the *effective dose equivalent* [6]) takes into account where the radiation dose is being absorbed (eg, which tissue has absorbed that radiation dose) and attempts to reflect the equivalent whole-body dose that results in a stochastic risk that is equivalent to the stochastic risk from the actual absorbed dose to those tissues irradiated in a non-uniform, partial-body irradiation such as a CT scan. It is a weighted average of organ doses, as described in Equation (1):

$$E = \sum_T (w_T \cdot w_R \cdot D_{T,R}), \quad (1)$$

where E is the effective dose, w_T is the tissue-weighting factor, w_R is the radiation-weighting coefficient (1 for x rays), $D_{T,R}$ is the average absorbed dose to tissue T , T is the subscript for each radiosensitive tissue, and R is the subscript for each type of radiation (here, only x rays are present). The weighting factors are set for each radiosensitive organ in Publication 60 of the International Commission on Radiological Protection (ICRP) (4). Effective dose is measured in sieverts (Sv) or rems. The conversion between sieverts and rems is $100 \text{ rem} = 1 \text{ Sv}$.

Although methods to calculate the effective dose have been established (ICRP Publications 26 [6] and 60 [4]), these methods depend heavily on the ability to estimate the dose to radiosensitive organs from the CT procedure ($D_{T,R}$). However, determining the radiation dose to these organs is problematic and direct measurement is not possible.

Radiation Dose

Measures: CT Specific

Because of its geometry and usage, CT is a unique modality and therefore has its own set of specific parameters for radiation dose (7–13). This modality is unique because the exposure is essentially continuous around the patient, rather than a projectional modality in which the exposure is taken from one or two source locations. The modality typically uses thin sections—ranging from 0.5-mm to 20-mm nominal beam collimation. However, this modality also typically uses multiple exposures along some length of the patient to cover a volume of anatomy. In addition,

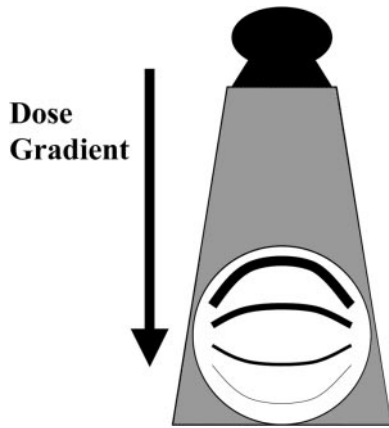


Figure 1. Dose gradient resulting from a projectional radiographic exposure in which the source is stationary at one position. The thicker lines represent the entrance skin dose, which is much larger than the exit skin dose, represented by the thinner lines. This difference creates a linear gradient through the patient.

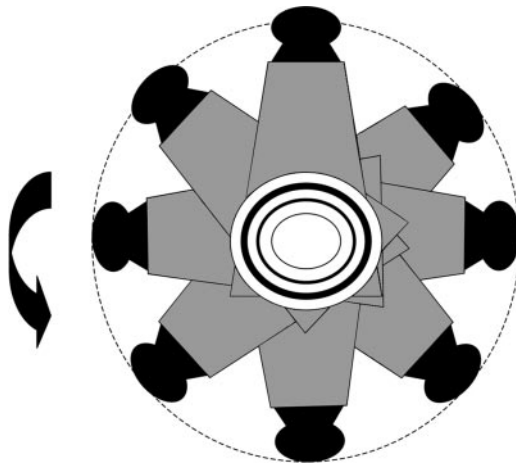


Figure 2. Dose gradient resulting from a full 360° exposure from a CT scan. The thicker lines represent the entrance skin dose, which is much larger than the dose at the inner radius, represented by the thinner lines. This difference results in a radially symmetric radiation dose gradient within the patient.

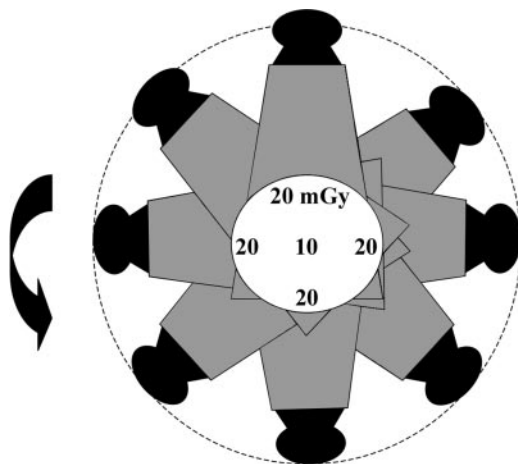


Figure 3. Typical dose measurements in a 32-cm-diameter (body) phantom from a single-detector CT scan. Values measured at the center and periphery (1 cm below the surface) positions within a polymethyl methacrylate circular dosimetry phantom demonstrate a radial dose gradient with a 2:1 ratio from periphery to center. Technical factors for the measurements were 120 kVp, 280 mA, 1-sec scan (ie, 280 mAs), and 10-mm collimation.

dose is much larger than the exit skin dose, creating a large radiation dose gradient across the patient (Fig 1). In contrast, the tomographic exposure of CT scans with a full 360° rotation results in a radially symmetric radiation dose gradient within the patient. That is, in a uniform circular object, such as a test phantom, all of the points at a certain radius from the center have the same (or nearly the same) radiation dose (Fig 2). As we shall see, the magnitude of that dose gradient (the size of the difference from center to periphery) will be affected by several factors, including the size of the object, the x-ray beam spectrum, and the attenuation of the material or tissue.

For example, in a typical CT dosimetry phantom that is 32 cm in diameter and made of polymethyl methacrylate (PMMA)—usually referred to as the *body phantom*—measurements of CT dose, which will be defined later, obtained at the center are typically about 50% of the measured value obtained at one of the peripheral positions. This result is illustrated in Figure 3, which shows the center value obtained under specific conditions to be approximately 10 mGy while the peripheral values are 20 mGy under those same conditions. However, for a smaller-diameter phantom—the 16-cm-diameter phantom referred to as the *head phantom*—measured under the identical exposure conditions, the center value reading climbs to approximately 40 mGy, as do

these exposures may be done in sequences of scans (eg, a series of scans such as pre- and post-contrast).

Variations within the Scan Plane

Projectional radiographic exposures are taken from one source position and the entrance skin

the peripheral values (Fig 4). This indicates that the magnitude of the difference from center to periphery is very much size dependent; it also indicates that the absolute values of the absorbed doses are size dependent.

Z-Axis Variations

In addition to the variations within the scan plane, there are variations along the length of the patient or phantom. These can be characterized by the z-axis dose distribution or radiation profile (Fig 5). This is the distribution of absorbed dose along the axis of the patient due to a single axial scan (a full rotation at one table position). The radiation profile is not limited to the primary area being imaged, and there are tails to this distribution from the nonideal collimation of the x-ray source and from scatter of photons within the object being exposed. When multiple adjacent scans are performed, the tails of the radiation profiles from adjacent scans can contribute to the absorbed dose outside of the primary area being imaged. If these tails are significant and are nonzero at some distance from the location of the originating section, then these contributions can add up, creating additional absorbed dose in the primary area being imaged.

That is, the radiation dose in a specific section consists of the sum of contributions to that section when that area is the primary area being imaged as well as the contributions from the tails of radiation profiles from adjacent sections when other locations are the primary area being imaged. The size of the contributions from adjacent sections is very directly related to the spacing of sections and the width and shape of the radiation profile.

To account for the effects from multiple scans, several dose descriptors were developed. One of the first was the Multiple Scan Average Dose (MSAD) descriptor (7,8,14). This is defined as the average dose resulting from a series of scans over an interval I in length:

$$\text{MSAD} = (1/I) \int_{-I/2}^{I/2} D_{\text{series}}(z) dz, \quad (2)$$

where I is the interval of the scan length and $D_{\text{series}}(z)$ is the dose at position z parallel to the z (rotational) axis resulting from the series of CT scans.

Following this was the Computed Tomography Dose Index (CTDI) (15). This was defined

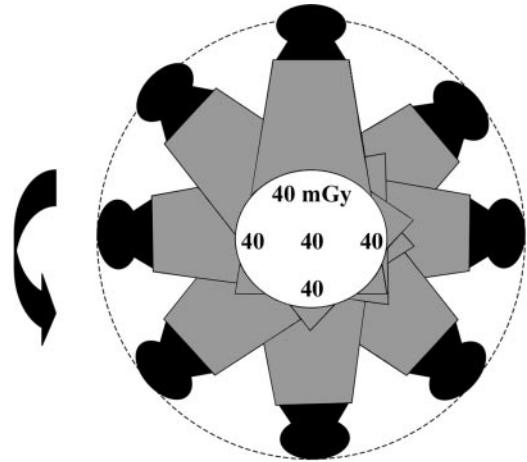


Figure 4. Typical dose measurements in a 16-cm-diameter (head) phantom from a CT scan. Values measured at the center and periphery (1 cm below the surface) positions within a polymethyl methacrylate circular dosimetry phantom demonstrate essentially no radial dose gradient. Technical factors for the measurements were 120 kVp, 300 mA, 1-sec scan (ie, 300 mAs), and 5-mm collimation.

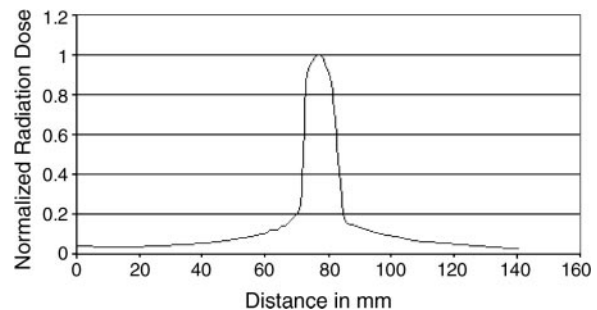


Figure 5. Radiation profile of a full-rotation CT scan measured at isocenter. This profile is the distribution of radiation dose along the axis of the patient (the z axis) and is known as $D(z)$.

as the radiation dose, normalized to beam width, measured from 14 contiguous sections:

$$\text{CTDI} = (1/nT) \int_{-7T}^{7T} D_{\text{single}}(z) dz, \quad (3)$$

where n is the number of sections per scan, T is the width of the interval equal to the selected section thickness, and $D_{\text{single}}(z)$ is the dose at point z on any line parallel to the z (rotational) axis for a single axial scan. This index was suggested by the Food and Drug Administration and incorporated into the Code of Federal Regulations (16).

However, to be measured according to the definition, only 14 sections could be measured and one had to measure the radiation dose profile—typically done with thermoluminescent dosimeters (TLDs) or film, neither of which was

very convenient. Measurements of exposure could be obtained with a pencil ionization chamber, but its fixed length of 100 mm meant that only 14 sections of 7-mm thickness could be measured with that chamber alone. To measure CTDI for thinner nominal sections, sometimes lead sleeves were used to cover the part of the chamber that exceeded 14 section widths.

To overcome the limitations of CTDI with 14 sections, another radiation dose index—CTDI₁₀₀—was developed. This index relaxed the constraint on 14 sections and allowed calculation of the index for 100 mm along the length of an entire pencil ionization chamber (14), regardless of the nominal section width being used. This index is therefore defined as follows (9):

$$CTDI_{100} = (1/NT) \int_{-5 \text{ cm}}^{5 \text{ cm}} D_{\text{single}}(z) dz, \quad (4)$$

where N is the number of acquired sections per scan (also referred to as the *number of data channels used during acquisition*) and T is the nominal width of each acquired section (which is not necessarily the same as the nominal width of the reconstructed section width).

(Note: The product of $N \cdot T$ is meant to reflect the total nominal width of the x-ray beam during acquisition. Therefore, if a multidetector scanner is used with four channels [rows] of 1.25 mm each for scan acquisition, then, regardless of the reconstructed section width, $NT = 4 \cdot 1.25 \text{ mm} = 5 \text{ mm}$; similarly, if the same scanner is used with four channels of 5-mm width for scan acquisition, then, regardless of the reconstructed section width, $NT = 20 \text{ mm}$.)

Because the ionization chamber measures an integrated exposure along its 100-mm length, this is equivalent to the following formula:

$$CTDI_{100} = (f \cdot C \cdot E \cdot L)/(NT), \quad (5)$$

where f is the conversion factor from exposure to a dose in air (use 0.87 rad/R), C is the calibration factor for the electrometer, E is the measured value of exposure in roentgens acquired from a single 360° rotation with a beam profile of NT (as defined earlier), L is the active length of the pencil ionization chamber, and N and T are as defined for Equation (4).

Thus, the exposure measurement, performed with one axial scan either in air or in one of the polymethyl methacrylate phantoms for which CTDI is defined, results in a calculated dose index, CTDI₁₀₀. This index can be measured and calculated for the center location as well as at least one of the peripheral positions (1 cm below

the surface) within the phantom to describe the variations within the scan plane as well.

CTDI_w was created to represent a dose index that provides a weighted average of the center and peripheral contributions to dose within the scan plane (9). This index is used to overcome the limitations of CTDI₁₀₀ and its dependency on position within the scan plane. The definition is as follows:

$$CTDI_w = (1/3)(CTDI_{100})_{\text{center}} + (2/3)(CTDI_{100})_{\text{periphery}}. \quad (6)$$

One final CTDI descriptor takes into account the parameters that are related to a specific imaging protocol, the helical pitch or axial scan spacing, and is defined as CTDI_{vol}:

$$CTDI_{\text{vol}} = CTDI_w \cdot NT/I, \quad (7)$$

where N and T are as defined earlier and represent the total collimated width of the x-ray beam and I is the table travel per rotation for a helical scan or the spacing between acquisitions for axial scans.

For helical scans, the following formulas are used:

$$NT/I = 1/\text{pitch} \quad (8)$$

and

$$CTDI_{\text{vol}} = CTDI_w/\text{pitch}, \quad (9)$$

where pitch is defined as table distance traveled in one 360° rotation/total collimated width of the x-ray beam.

Another dose descriptor that is related to CTDI and is commonly reported on CT scanners and in the literature is the dose-length product (DLP) (9). This value is simply the CTDI_{vol} multiplied by the length of the scan (in centimeters) and is given in units of milligray-centimeters:

$$DLP = CTDI_{\text{vol}} \cdot \text{scan length}. \quad (10)$$

This descriptor is used in one approach to obtain an estimate of effective dose that will be described later.

These CTDI descriptors are obviously meant to serve as an index of radiation dose due to CT scanning and are not meant to serve as an accurate estimate of the radiation dose incurred by an individual patient. Although the phantom

measurements are meant to be reflective of an attenuation environment somewhat similar to a patient, the homogeneous polymethyl methacrylate phantom does not simulate the different tissue types and heterogeneities of a real patient. In addition, the $CTDI_{100}$ calculation uses the f factor (from Eq [5]) only to convert from exposure to a dose in air; other tissues have different f factors. The f factor (in units of rads per roentgen) is determined by the ratio of the mass energy absorption coefficient of a tissue to that of air:

$$f = 0.87 \cdot [(\mu_t/\rho_t)/(\mu_a/\rho_a)], \quad (11)$$

where μ_t/ρ_t is the mass energy absorption coefficient of the tissue (eg, bone, lung, soft tissue) and μ_a/ρ_a is the mass energy absorption coefficient of air. The mass energy absorption coefficient depends not only on the tissue but also on the energy of the photons, especially in the energy range used by CT. Thus, the $CTDI_{100}$ calculation presents a very simplified condition for measuring radiation dose.

Factors That Influence Radiation Dose from CT

In general, there are some factors that have a direct influence on radiation dose, such as the x-ray beam energy (kilovolt peak), tube current (in milliamperes), rotation or exposure time, section thickness, object thickness or attenuation, pitch and/or spacing, dose reduction techniques such as tube current variation or modulation, and distance from the x-ray tube to isocenter. In addition, there are some factors that have an indirect effect on radiation dose—those factors that have a direct influence on image quality, but no direct effect on radiation dose; for example, the reconstruction filter. Choices of these parameters may influence an operator to change settings that do directly influence radiation dose. These factors are discussed in this section.

Beam Energy

The energy of the x-ray beam has a direct influence on patient radiation dose. This is selected by the operator (technologist) when the kilovolt peak is chosen for the scan. However, it is also influenced by the filtration selected for the scan. On some scanners, the selection of filtration is explicit; for others, it is implied (eg, by selection of the scan field of view [SFOV]). The influence of beam energy is shown in Table 1. When all other technical parameters are held constant and the

Table 1
Changes in $CTDI_w$ in Head and Body Phantoms as a Function of Kilovolt Peak

Beam Energy (kVp)	$CTDI_w$ in Head Phantom (mGy)	$CTDI_w$ in Body Phantom (mGy)
80	14	5.8
100	26	11
120	40	18
140	55	25

Note.—All other factors were held constant at 300 mA, 1 sec, and 10 mm. Results are from a single-detector CT scanner.

Table 2
Changes in $CTDI_w$ in Head and Body Phantoms as a Function of Milliampere-Seconds Setting

Tube Current–Time Product (mAs)	$CTDI_w$ in Head Phantom (mGy)	$CTDI_w$ in Body Phantom (mGy)
100	13	5.7
200	26	12
300	40	18
400	53	23

Note.—All other factors were held constant at 120 kVp and 10 mm. Results are from a single-detector CT scanner.

kilovolt peak is increased on a single-detector CT scanner, the $CTDI_w$ values also increase for both the head and body $CTDI$ phantoms. For example, when the kilovolt peak was increased from 120 to 140 on a CT/i scanner (GE Medical Systems, Milwaukee, Wis), the $CTDI_w$ increase was 37.5% for the head phantom and 39% for the body phantom.

Photon Fluence

The photon fluence, as influenced by the tube current–time product (milliampere-seconds), also has a direct influence on patient radiation dose. As one might expect, the radiation dose is directly proportional to the milliampere-seconds value. This is shown in Table 2, which gives the results when the milliampere-seconds value is increased and all other technical parameters are held constant on a single-detector CT scanner. Under these conditions, the $CTDI_w$ values increase linearly with milliampere-seconds for both the head and body $CTDI$ phantoms.

Table 3
Changes in CTDI_{vol} in Head and Body Phantoms as a Function of Pitch

Pitch	CTDI _{vol} in Head Phantom (mGy)	CTDI _{vol} in Body Phantom (mGy)
0.5	80	36
0.75	53	24
1.0	40	18
1.5	27	12
2.0	20	9

Note.—All other factors were held constant at 120 kVp, 300 mA, 1 sec, and 10 mm. Results are from a single-detector CT scanner.

Table 4
Changes in CTDI_w in Head and Body Phantoms as a Function of Collimation for a Single-Detector Scanner

Collimation (mm)	CTDI _w in Head Phantom (mGy)	CTDI _w in Body Phantom (mGy)
1	45	19
3	41	18
5	40	18
7	40	18
10	40	18

Note.—All other factors were held constant at 120 kVp and 300 mAs.

Note that these results hold only while the tube current–time product is varied and all other parameters are held constant. This is an issue because on some scanners, the user inputs a parameter labeled “mAs,” but that parameter is really the *effective* milliamperere-seconds value, which is milliamperage · time/pitch. On these scanners, when pitch is varied, the milliamperere-seconds value is varied in a corresponding fashion to keep the effective milliamperere-seconds value constant (17). The effects of pitch are discussed in the next section.

Helical Pitch

For helical scans, the pitch parameter (defined as table distance traveled in one 360° rotation/total collimated width of the x-ray beam) has a direct influence on patient radiation dose. This is essentially because as pitch increases, the time that any one point in space spends in the x-ray beam is decreased. The relationship between radiation dose and pitch has been shown previously by us-

ing phantoms and thermoluminescent dosimeters (18). On the basis of these results, the CTDI_{vol} (which is the only CTDI descriptor that takes pitch into account) varies as shown in Table 3, which gives the results when the pitch is varied and all other technical parameters are held constant on a single-detector CT scanner.

X-ray Beam Collimation: Single-Detector Scanners

The collimation of the x-ray beam will both directly and indirectly influence the patient radiation dose. The indirect effects will be described later. For a single section with all other technical parameters held constant, more x-ray photons will be transmitted when the collimator setting is wider (wider x-ray beam for a thicker section). However, exposure and absorbed radiation dose are defined on a per unit mass basis. The thicker section has more photons available but also more mass being irradiated than a thinner section, thus indicating that the radiation dose for thick and thin sections may be close to equivalent (the difference might be attributed to the higher scatter expected in the thicker section). This equivalence would also assume that the radiation profiles (and, as shown earlier, the overlap between adjacent exposures) are equivalent between narrow and wide collimation settings. However, previous publications have shown that this is not quite true for single-detector scanners and that thinner collimations typically result in a greater degree of overlap and higher CTDI values (18). The results from measuring CTDI_w are shown in Table 4, which gives the results when the collimation is varied and all other technical parameters are held constant on a single-detector CT scanner.

X-ray Beam Collimation: Multiple-Detector Scanners

Although the effects of beam collimation were small for a single-detector scanner, current experience shows that this is not the case with multidetector scanners. In fact, early reports from early versions of multidetector scanners showed significant dependence on x-ray beam collimation (19). These effects result from differences in x-ray beam collimation—even when the same reconstructed section thickness is used. That is, on many multidetector scanners, there are several ways to scan and reconstruct images that have the same section thickness. For example, on one multidetector CT scanner (LightSpeed Qx/i; GE Medical Systems), one can perform axial scans of

4 × 1.25 mm (5-mm beam width), 4 × 2.5 mm (10-mm beam width), and 4 × 5 mm (20-mm beam width) to make a 5-mm-thick reconstructed section. For each of these modes, when CTDI_w values are measured, there is a surprising difference in absorbed dose. These results are shown in Table 5, which gives the results when all other technical parameters are held constant on that multidetector CT scanner.

These results show that the difference in beam collimation, not the reconstructed section width, makes a significant difference in CTDI_w. These differences may be as much as 55% in the head phantom and 65% in the body phantom, with the higher doses coming when narrower beam collimation is used.

Effects of Object (and Patient) Size

In each of the preceding sections, we reported results for both the head and body phantoms. These phantoms, as described earlier, are made of the same soft-tissue–equivalent material but are 16-cm-diameter and 32-cm-diameter right circular cylinders, respectively. To produce each table, we used the same technical factors for each phantom. Therefore, the primary difference in results between the head and body phantoms is size. Each of the tables shows that when the same technical parameters are used, the appropriate index shows that the smaller object always absorbs the higher dose and that the difference is at least a factor of two. Thus, for the same exposure factors, smaller patients would be expected to absorb much higher amounts of radiation dose than larger patients. This has significant implications for pediatric patients and small adults.

This is primarily because tissues are being exposed with both entrance radiation (as the tube is positioned directly over the tissue) and exit radiation (as the tube moves to the other side of the patient) as the source moves around the patient. For smaller patients, the exit radiation has been attenuated by less tissue and therefore is closer to the entrance radiation in its intensity, resulting in a much more uniform dose distribution (nearly equal at all locations in a 16-cm-diameter phantom). For the larger patient, the exit radiation is much less intense due to its attenuation through more tissue. This results in a difference within the scan plane with the higher radiation dose values occurring near the periphery, where entrance exposure is highest.

The effect of patient or object size on radiation dose has brought significant discussion into the proper selection of protocols for imaging pediatric

Table 5
Changes in CTDI_w in Head and Body Phantoms as a Function of Collimation for a Multidetector Scanner

Collimation (mm)	Total Beam Width (mm)	CTDI _w in Head Phantom (mGy)	CTDI _w in Body Phantom (mGy)
4 × 1.25	5	62	33
2 × 2.5	5	62	33
1 × 5	5	62	33
4 × 2.5	10	46	24
2 × 5	10	46	24
4 × 5	20	40	20

Note.—All other factors were held constant at 120 kVp and 300 mAs.

patients as well as adjusting technical factors for patients according to size (20–28).

Other Options for Reducing Scan Dose

In addition to the technical parameters discussed earlier, manufacturers have recently provided users with other means to reduce patient dose. One of these is an option to make changes in tube current based on the estimated attenuation of the patient at a specific location. Thus, the tube current will be programmed to a maximum value and can be reduced when there is information that a location along the patient is expected to be less attenuating than the most attenuating location to be imaged. This is determined by using both anteroposterior and lateral planning projection views. From these views, the tube current will be programmed to vary by location along the length of the patient and even as the tube is rotating around the patient. The exact details of the option vary by manufacturer.

In the near future, manufacturers may provide real-time (or close to real-time) tube current modulation (29–31), so that tube current can be varied (reduced) as the scan is actually occurring, eliminating the need for both planning projections for dose reduction purposes (they may still be needed for planning purposes).

Indirect Effects

In addition to the direct effects that collimation has, as described earlier, there are some indirect effects that both it and the reconstruction algorithm may have on radiation dose. This is because, when thinner reconstructed image thicknesses are used, with all other factors held constant, there will be more noise in the image (where noise is defined as the standard deviation of the CT number). Therefore, noise typically

increases with $1/\sqrt{T}$, where T is the nominal section thickness. Therefore, a 10-mm-thick section is expected to have 3.2 times less noise than a 1-mm-thick section. Often when noisy images are obtained, the kilovolt peak or milliampere-seconds value or both are increased to offset the increase in noise due to narrower sections. Similar behavior is observed for the effects of the reconstruction algorithm. Algorithms that enhance higher spatial frequencies and improve spatial resolution (such as required for lung or skeletal imaging) also increase the noise in the image. To overcome this increase in noise, the kilovolt peak or milliampere-seconds value or both may be increased. This increase in kilovolt peak or milliampere-seconds value will result in an increase in radiation dose. Therefore, although changing the algorithm or section thickness may not have a direct effect on radiation dose, the selection of technical factors to offset the resulting increase in image noise may result in an increase in radiation dose.

Methods to Reduce Patient Dose

From the preceding discussion, it appears that there are several mechanisms to reduce the radiation dose to a patient (32,33). However, each of them has some resulting trade-off involved. Each of these is discussed below (27).

Reducing the Milliampere-Seconds Value.—

From the results presented earlier, the radiation dose is linear with the milliampere-seconds value when all other factors are held constant. So, if the milliampere-seconds value is reduced by 50%, the radiation dose will be reduced by the same amount. However, this reduction will increase image noise by $1/\sqrt{\text{mAs}}$, which means that a 50% reduction in the milliampere-seconds value results in a noise increase of 41% ($1/\sqrt{2} = 1.41$, a 41% increase). Depending on the requirements of the clinical application, this reduction may be readily accepted; in other cases, this type of reduction in milliampere-seconds may compromise the diagnostic quality of the imaging examination. For example, detection of high-contrast objects in the lung may not require a low-noise imaging protocol and the reduction in milliampere-seconds may be well tolerated. On the other hand, imaging low-contrast lesions in the liver does require a low-noise imaging protocol and the reduction in milliampere-seconds may limit the ability to detect these lesions.

Increasing Pitch.—The radiation dose is inversely proportional to pitch when all other factors are held constant. Therefore, increasing pitch is one consistent way to reduce radiation dose. The trade-off in increasing pitch is an increase in

effective section thickness, which results in increased volume averaging, which in turn may reduce the image signal (contrast between some object and background). The ability to use this type of dose reduction again depends on the clinical application.

Varying the Milliampere-Seconds Value by Patient Size.—CT is an example of a digital modality in which the image quality continues to improve as the exposure increases. This is contrasted with analog projectional film, in which too high of an exposure results in an overexposed (too dark) film. Thus, when pediatric patients or small adult patients are imaged with CT using full-sized adult techniques, there is no penalty to image quality; in fact, the image quality is better under these conditions, as more photons reach the detector and image noise is reduced. However, the radiation dose to the smaller patient is potentially higher than is necessary to obtain a diagnostic image. Therefore, significant effort has recently been put into developing size- and weight-based imaging protocols to reduce radiation dose to pediatric patients and small adult patients, so that radiation dose can be reduced while still achieving sufficient diagnostic image quality (21–25,27). This has typically been in the form of a reduced milliampere-seconds value for reduced patient size and has led to the development of suggested technique charts for pediatric patients.

Reducing Beam Energy.—As discussed earlier, reducing the beam energy results in reduced radiation dose when all other factors are held constant. This will increase the image noise, and contrast changes will occur with a change in kilovolt peak, increasing with lower kilovolt peak for most tissue interfaces but decreasing or changing very little for others. From CTDI_{100} results, and *not* from the CTDI_w results, we can observe that the radiation dose gradient is larger from periphery to center in the body phantom at lower kilovolt peak settings. This implies a greater relative skin dose for patients when lower kilovolt peak settings are used.

Estimating Effective Dose from CT

The definition of effective dose was given earlier (Eq [1]) (4) as the weighted sum of organ doses resulting from the examination, where the radio-sensitive organs were defined along with their tissue-weighting factors. Although it appears straightforward to estimate effective dose, it is

actually difficult to accurately estimate the dose to an individual organ from a CT scan. This is even more difficult when attempting to estimate the effective dose for each patient when each one has unique characteristics of height, weight, age, gender, and composition. Still, several different methods for estimating effective dose—primarily to standard patient models—have been developed.

The first is based on Monte Carlo simulations performed several years ago (34–37). This work, performed by members of the United Kingdom's National Radiological Protection Board (NRPB), used Monte Carlo methods to simulate CT scanning around a previously developed mathematical patient model (MIRD V [38]). This hermaphrodite patient model uses geometric shapes (cylinders, spheres, cones) to approximate the shape and location of all radiosensitive organs in the body; other approximations were used for the brain and lens of the eye. Physical measurements of CTDI in air on many scanners were collected as part of a national dosimetry program (36); these data were used to convert from the normalized Monte Carlo data to absolute dose values. The simulation also involved modeling scanner geometry, spectrum, section thickness, and other properties with the patient model in the beam—accounting for primary and scatter radiation. From these simulations, radiation doses for each organ in each imaged section were calculated and could be tallied to estimate the organ dose for each organ. These organ doses could then be combined with appropriate weighting factors to estimate effective dose (or effective dose equivalent from ICRP 26). This work was completed before helical and multidetector scanners were commonplace and did not explicitly model helical scanning or the effects of multidetector scanners.

This work formed the basis for several software programs that have taken the results of these simulations and put an interface on them to allow users to input some technical parameters and calculate an effective dose. These include programs such as CTDOSE (from John Le Heron at New Zealand's National Radiation Laboratory [johnleh@nrl.moh.govt.nz]) and the Microsoft (Redmond, Wash) Excel-based product from the Imaging Performance Assessment of CT (IMPACT) scanners group in the United Kingdom (39). The latter software package matches the desired scanner to one of those used in the original study on the basis of CTDI in air as well as CTDI in phantom measurements.

In a related but independent effort, Zankl et al (40) from the Gesellschaft für Strahlen- und Um-

weltforschung (GSF) performed simulations on two different mathematical sex-specific phantoms, "Adam" and "Eva" (41), which were based on the ICRP data on Reference Man. Similar to the MIRD V phantom, the GSF mathematical phantoms were described by using combinations of spheres, ellipsoids, cones, and parts and combinations of these shapes. The Monte Carlo simulations were performed modeling photon transport through the simulated patient by using three different energy spectra. The section thickness was 1 cm, and radiation doses were calculated for single sections at positions varying contiguously from the bottom of the trunk to the top of the head. The result was mean organ conversion factors for each organ and per single CT section of 1 cm width centered at a given location in the phantom. The mean dose to a single organ resulting from a particular CT scan was estimated by summing up the contribution to the organ dose from each relevant section. The relative organ doses were converted to absolute organ doses by using the air kerma free-in-air on the axis of rotation. As in the National Radiological Protection Board data, these organ doses can be combined with appropriate weighting factors to estimate effective dose (or effective dose equivalent from ICRP 26).

The GSF work formed the basis for a software program with a graphical user interface (42). This package (WinDose; Scanditronix/Wellhofer, Schwarzenbruck, Germany, www.wellhofer.com) has taken the results of the simulations and put an interface on them to allow users to input some technical parameters and calculate an effective dose. The output is an estimate of the effective dose given the scanner characteristics, body region, scan range, and other parameters. This program also outputs the effective dose in millisieverts as well as in units of natural background radiation per year.

Another approach was that of estimating the energy imparted, developed by Atherton and Huda (43–47). Energy imparted is the measure of the total ionizing energy deposited in the patient during the CT examination and here is symbolized by ϵ . On the basis of the simulation data of Jones and Shrimpton (36,37), the energy imparted was calculated for a mathematical anthropomorphic phantom (38). For different CT systems, the ratio of effective dose equivalent (H_E , defined in ICRP 26 [6]) to energy imparted (H_E/ϵ) and the ratio of effective dose (E , defined in ICRP 60 [4]) to energy imparted (E/ϵ) were calculated and plotted as a function of the position along the anthropomorphic phantom. High peaks in this function showed the position of organs with a higher radiosensitivity like the gonads, breast, or thyroid. Therefore, in this approach,

effective dose is estimated by first estimating the energy imparted to the body region being scanned and then multiplying by the ratio factor for that particular region.

One other method of note to estimate the effective dose involves conversion factors for a general anatomic region as described by the European Guidelines on Quality Criteria for Computed Tomography (9), which are based on the work of Jessen et al (48). In this approach, the $CTDI_{vol}$ and distance are used to estimate the DLP, which is then multiplied by a region-specific conversion factor to estimate the effective dose. These conversion factors range from 0.0023 mSv/mGy · cm for the head region to 0.017 mSv/mGy · cm for the chest region and 0.019 mSv/mGy · cm for the pelvis. This approach obviously does not take into account any patient-specific or even examination-specific factors but provides an easily estimated value of effective dose.

For a typical chest scan performed with a single-detector scanner at 120 kVp, 250 mAs, 5–7-mm collimation, and a pitch of 1, the $CTDI_{100, center}$ would be 10 mGy, the $CTDI_{100, periphery}$ would be 18 mGy, the $CTDI_w$ would be 15 mGy, and the $CTDI_{vol}$ would be 15 mGy. If a length of scan of 25 cm is assumed, the DLP would be 375 mGy · cm; when the conversion factor for the chest is used, one estimate of effective dose would be 6.4 mSv.

For a typical head scan performed with a single-detector scanner at 120 kVp, 300 mAs, 5-mm collimation, and a pitch of 1, the $CTDI_{100, center}$ would be 40 mGy, the $CTDI_{100, periphery}$ would be 40 mGy, the $CTDI_w$ would be 40 mGy, and the $CTDI_{vol}$ would be 40 mGy. If a length of scan of 17.5 cm is assumed, the DLP would be 700 mGy · cm; when the conversion factor for the head is used, one estimate of effective dose would be 1.6 mSv. Thus, the effective dose for the head scan is considerably less than that for the chest scan, even though the CTDI values for the head scan are much higher. This is because fewer of the radiosensitive organs are irradiated.

Relevant Activities and Resources

There have been recent activities regarding radiation dose in many different agencies and organizations. These include an ongoing focus on radiation dose by the Society for Pediatric Radiology, where the dose from CT to pediatric patients is an issue of significant concern. These concerns were presented in several articles including references 20–28, which reflected the concern that CT techniques being used for pediatric patients were similar to those used for adults and were not being adapted to the small size of pediatric patients. These articles also reported that pediatric

patients may have increased sensitivity to ionizing radiation. Since that time, the Society for Pediatric Radiology has held sessions at its annual conferences dedicated to CT and radiation dose reduction techniques.

The American Association of Physicists in Medicine (AAPM) has convened a task group (Task Group 23: CT Dosimetry) under its Diagnostic X-ray Imaging Committee to address issues related to CT radiation dose. This task group is addressing issues relating to standardizing descriptors, measurement methods, and education activities related to these. This is in addition to the task group on reference values created under the AAPM's Radiation Protection Committee (Task Group 7: Reference Values for Diagnostic X-ray Examinations), which reports values for head CT scans. Both of these task groups operate under the AAPM's Science Council.

In addition, the CT accreditation program of the American College of Radiology (ACR) requires sites applying for accreditation to measure and calculate $CTDI_{100}$, $CTDI_w$, $CTDI_{vol}$, DLP, and effective dose for pediatric body, adult head, and adult body techniques. Although this will not be a pass-fail criterion at first, the ACR's program will eventually use radiation dose as part of its pass-fail criteria. This program does provide acceptable value limits for each protocol.

The Center for Devices and Radiological Health (CDRH) of the Food and Drug Administration has made some public recommendations on CT scanning for pediatric and small adult patients, which they have published on their Web site (27). In addition, the agency has completed its Nationwide Evaluation of X-ray Trends (NEXT) for CT, which was undertaken in 2000 (1). Preliminary results were presented at the 2001 conference of the Radiological Society of North America. In this survey, CTDI values were reported from many different scanners placed at different institutions across the United States. From this survey, mean values as well as ranges of values are being obtained for different types of scans. Publications on the results of this survey are being prepared.

Conclusions

This article describes the basic concepts of radiation dose in CT. The basic concepts of exposure, absorbed dose, and effective dose were described in general and then described in the context of CT-specific descriptors. The various CTDI descriptors were defined, and the relationships between them were described as well. Once these

CTDI parameters were defined, factors that influence radiation dose, both directly and indirectly, were described and the magnitudes of those effects were reported. The effective dose was described, and several methods for estimating this important parameter were presented. Some relevant activities were identified.

Although there are many dose descriptors and methods for measuring radiation dose and effective dose from CT, there are still areas for further research. Recent investigations include examining the effects of patient size on radiation dose (with specific implications for pediatric patients) and methods for estimating patient-specific radiation dose (49,50), rather than estimating based on phantoms or standard mathematical patients such as the MIRD V. In the near future, there may be methods to estimate the radiation dose, organ dose, and effective dose from arbitrary CT scanning protocols by using patient-specific models.

References

1. Stern SH, Kaczmarek RV, Spelic DC, Suleiman OH. Nationwide Evaluation of X-ray Trends (NEXT) 2000–2001 survey of patient radiation exposure from computed tomographic (CT) examinations in the United States (abstr). *Radiology* 2001; 221(P):161.
2. Center for Devices and Radiological Health, Food and Drug Administration. Whole body scanning using computed tomography (CT). Available at: <http://www.fda.gov/cdrh/ct/>. Accessed April 2002.
3. Bushberg JT, Seibert JA, Leidholdt EM, Boone JM. The essential physics of medical imaging. 2nd ed. Philadelphia, Pa: Lippincott Williams & Wilkins, 2001.
4. International Council on Radiation Protection. 1990 recommendations of the International Commission on Radiological Protection. Publication 60, *Annals of the ICRP* 1991; 21. Oxford, England: Pergamon, 1991.
5. McCollough CM, Schueler BA. Calculation of effective dose. *Med Phys* 2000; 27:838–844.
6. International Council on Radiation Protection. Recommendations of the International Commission on Radiological Protection, 1977. Publication 26, *Annals of the ICRP* 1(3) (reprinted with additions in 1987). Oxford, England: Pergamon, 1977. [superseded by ICRP Publication 60]
7. American Association of Physicists in Medicine. Standardized methods for measuring diagnostic x-ray exposure. Report no. 31, 1990. Available at: www.aapm.org/pubs/reports.
8. American Association of Physicists in Medicine. Specification and acceptance testing of computed tomography scanners. Report no. 39, 1993. Available at: www.aapm.org/pubs/reports.
9. European Guidelines on Quality Criteria for Computed Tomography (EUR 16262 EN, May 1999). Available at: www.drs.dk/guidelines/ct/quality/index.htm. Accessed July 2002.
10. Shrimpton PC, Edyvean S. CT scanner dosimetry. *Br J Radiol* 1998; 71:1–3.
11. Rothenberg LN, Pentlow KS. CT dosimetry and radiation safety. In: Goldman LW, Fowlkes JB, eds. *Syllabus: a categorical course in diagnostic radiology physics—CT and US cross-sectional imaging*. Oak Brook, Ill: Radiological Society of North America, 2000; 171–188.
12. McCollough CM, Zink FE. Performance evaluation of CT systems. In: Goldman LW, Fowlkes JB, eds. *Syllabus: a categorical course in diagnostic radiology physics—CT and US cross-sectional imaging*. Oak Brook, Ill: Radiological Society of North America, 2000; 189–207.
13. Nagel HD, ed. *Radiation exposure in computed tomography*. 2nd ed. Hamburg, Germany: CO-CIR, 2000. [available through cocir@zvei.org]
14. Jucius RA, Kambic GX. Radiation dosimetry in computed tomography. *Appl Opt Instrum Eng Med* 1977; 127:286–295.
15. Shope TB, Gagne RM, Johnson GC. A method for describing the doses delivered by transmission x-ray computed tomography. *Med Phys* 1991; 8:488–495.
16. Department of Health and Human Services, Food and Drug Administration. 21 CFR Part 1020: Diagnostic x-ray systems and their major components; amendments to performance standard; Final rule. *Federal Register* 1984, 49, 171.
17. Mahesh M, Scatarige JC, Cooper J, Fishman EK. Dose and pitch relationship for a particular multi-slice CT scanner. *AJR Am J Roentgenol* 2001; 177:1273–1275.
18. McNitt-Gray MF, Cagnon C, Solberg TD, Chetty I. Radiation dose from spiral CT: the relative effects of collimation and pitch. *Med Phys* 1999; 26:409–414.
19. McCollough CH, Zink FE. Performance evaluation of a multi-slice CT system. *Med Phys* 1999; 26:2223–2230.
20. Brenner DJ, Elliston CD, Hall EJ, Berdon WE. Estimated risks of radiation-induced fatal cancer from pediatric CT. *AJR Am J Roentgenol* 2001; 176:289–296.
21. Paterson A, Frush DP, Donnelly LF. Helical CT of the body: are settings adjusted for pediatric patients? *AJR Am J Roentgenol* 2001; 176:297–301.
22. Donnelly LF, Emery KH, Brody AS, et al. Perspective: minimizing radiation dose for pediatric body applications of single-detector helical CT—strategies at a large children's hospital. *AJR Am J Roentgenol* 2001; 176:304–306.
23. Robinson AE, Hill EP, Harpen MD. Radiation dose reduction in pediatric CT. *Pediatr Radiol* 1986; 16:53–54.
24. Kamel IR, Hernandez RJ, Martin JE, Schlesinger AE, Niklason LT, Guire KE. Radiation dose reduction in CT of the pediatric pelvis. *Radiology* 1994; 190:683–687.
25. Rogalla P, Stöver B, Scheer I, Juran R, Gaedicke G, Hamm B. Low-dose spiral CT: applicability to paediatric chest imaging. *Pediatr Radiol* 1998; 29:565–569.
26. Huda W, Chamberlain CC, Rosenbaum AE, Garisi W. Radiation doses to infants and adults undergoing head CT examinations. *Med Phys* 2001; 28:393–399.

27. Feigal DW. FDA Public Health Notification: reducing radiation risk from computed tomography for pediatric and small adult patients. Center for Devices and Radiological Health, Food and Drug Administration. Available at: <http://www.fda.gov/cdrh/safety/110201-ct.html>. Accessed November 2001.
28. Shrimpton PC, Wall BF. Reference doses for paediatric computed tomography. *Radiat Prot Dosimetry* 2000; 90:249–252.
29. Gies M, Suess C, Wolf H, Kalender WA, Madsen MT. Dose reduction in CT by anatomically adapted tube current modulation. I. Simulation studies. *Med Phys* 1999; 26:2235–2247.
30. Kalender WA, Wolf H, Suess C, Gies M, Bautz WA. Dose reduction in CT by anatomically adapted tube current modulation. II. Phantom measurements. *Med Phys* 1999; 26:2248–2253.
31. Kalender WA, Wolf H, Suess C, Gies M, Greess H, Bautz WA. Dose reduction in CT by on-line tube current control: principles and validation on phantoms and cadavers. *Eur Radiol* 1999; 9:323–328.
32. Ravenel JG, Scalzetti EM, Huda W, Garrisi W. Radiation exposure and image quality in chest CT examinations. *AJR Am J Roentgenol* 2001; 177:279–284.
33. Huda W, Scalzetti EM, Levin G. Technique factors and image quality as functions of patient weight at abdominal CT. *Radiology* 2000; 217:430–435.
34. Shrimpton PC, Jones DG, Hillier MC, Wall BF, Le Heron JC, Faulkner K. Survey of CT practice in the UK. Part 2: Dosimetric aspects. NRPB R249. Chilton, England: National Radiological Protection Board, 1991.
35. Jones DG, Shrimpton PC. Survey of CT practice in the UK. Part 3: Normalised organ doses calculated using Monte Carlo techniques. NRPB R-250. Chilton, England: National Radiological Protection Board, 1992.
36. Jones DG, Shrimpton PC. Normalised organ doses for x-ray computed tomography calculated using Monte Carlo techniques. NRPB SR-250. Chilton, England: National Radiological Protection Board, 1992. [computer software report]
37. Shrimpton PC, Jones DG. Normalised organ doses for x-ray computed tomography calculated using Monte Carlo techniques and a mathematical anthropomorphic phantom. *Radiat Prot Dosimetry* 1993; 49:241–243.
38. Cristy M. Mathematical phantoms representing children of various ages for use in estimates of internal dose. NUREG/CR-1159 ORNL/NUREG/TM-367. Oak Ridge, Tenn: Oak Ridge National Laboratory, 1980.
39. Imaging Performance Assessment of CT (IMPACT) CT Patient Dosimetry Calculator, version 0.99m. Created 07/01/2002. Available at: <http://www.impactscan.org/ctdosimetry.htm>.
40. Zankl M, Panzer W, Drexler G. The calculation of dose from external photon exposures using reference human phantoms and Monte Carlo methods. Part VI: Organ doses from computed tomographic examinations. GSF-Bericht 30/91. Neuherberg, Germany: Gesellschaft für Strahlen- und Umweltforschung, 1991.
41. Kramer R, Zankl M, Williams G, Drexler G. The calculation of dose from external photon exposures using reference human phantoms and Monte Carlo methods. Part I: The male (Adam) and female (Eva) adult mathematical phantoms. GSF-Bericht S-885. Munich, Germany: Gesellschaft für Strahlen- und Umweltforschung, 1982.
42. Kalender WA, Schmidt B, Zankl M, Schmidt M. A PC program for estimating organ dose and effective dose values in computed tomography. *Eur Radiol* 1999; 9:555–562.
43. Atherton JV, Huda W. CT doses in cylindrical phantoms. *Phys Med Biol* 1995; 40:891–911.
44. Huda W, Atherton JV. Energy imparted in computed tomography. *Med Phys* 1995; 22:1263–1269.
45. Atherton JV, Huda W. Energy imparted and effective doses in computed tomography. *Med Phys* 1996; 23:735–741.
46. Huda W, Scalzetti EM, Roskopf M. Effective doses to patients undergoing thoracic computed tomography examinations. *Med Phys* 2000; 27:838–844.
47. Ware DE, Huda W, Mergo PJ, Litwiller AL. Radiation effective doses to patients undergoing abdominal CT examinations. *Radiology* 1999; 210:645–650.
48. Jessen KA, Shrimpton PC, Geleijns J, Panzer W, Tois G. Dosimetry for optimisation of patient protection in computed tomography. *Appl Radiat Isot* 1999; 50:165–172.
49. Beifuss U, McNitt-Gray MF, Cagnon CH, DeMarco JJ. Monte Carlo methods to simulate radiation dose from spiral computed tomography: phantom studies (abstr). *Radiology* 2000; 217(P):488.
50. Jarry G, DeMarco JJ, McNitt-Gray MF. Monte Carlo dose verification of a commercial CT scanner with applications for patient specific dosimetry (abstr). *Med Phys* 2002; 29:1344. [presented at the 2002 annual conference of the American Association of Physicists in Medicine]